NETWORKS AND HETEROGENEOUS MEDIA
©American Institute of Mathematical Sciences
Volume **1**, Number **1**, March **2006**
Website: http://aimSciences.org
pp. **143–166**

NUMERICAL STUDY OF A DOMAIN DECOMPOSITION METHOD FOR A TWO-SCALE LINEAR TRANSPORT EQUATION

Xu Yang

Department of Mathematical Sciences, Tsinghua University
Beijing 100084, P.R. China
Current address: Department of Mathematics, University of Wisconsin
Madison, WI 53706, USA

Francois Golse

Institut Universitaire de France & Département de Mathé- matiques et Applications
Ecole Normale Supérieure Paris, 45 rue d'Ulm, 75230 Paris cedex 05, France

Zhongyi Huang

Department of Mathematical Sciences, Tsinghua University
Beijing 100084, P.R. China

Shi Jin

Department of Mathematics, University of Wisconsin
Madison, WI 53706, USA
and Department of Mathematical Sciences, Tsinghua University
Beijing 100084, P.R. China

Abstract. We perform a numerical study on a domain decomposition method proposed in [13] for the linear transport equation between a diffusive and a non-diffusive region. This method avoids iterating the diffusion and transport solutions as in a typical domain decomposition method. Our numerical results, in both one and two space dimensions, confirm the theoretical analysis of [13]. We also provide an improved second order method that provides a more accurate numerical solution than that proposed in [13].

1. **Introduction.** Consider the steady, linear transport equation with isotropic scattering and slab geometry:

$$\mu\partial_x\Psi(x,\mu)+\sigma(x)\Psi(x,\mu)=\sigma(x)c(x)\overline{\Psi}(x)\,,$$
$$\text{where } \overline{\Psi}(x)=\frac{1}{2}\int_{-1}^{1}\Psi(x,\mu)d\mu\,. \tag{1.1}$$

The phase space density Ψ is defined so that $\Psi(x,\mu)\frac{1}{2}d\mu dx$ is the number of particles (e.g. neutrons) located inside an interval of width dx centered at x, moving in a direction whose angle θ with the x axis is such that $\mu=\cos\theta$ belongs to an interval

2000 *Mathematics Subject Classification.* 35B25, 65M60, 76R50, 82C70 .

Key words and phrases. linear transport equation, diffusion approximation, domain decomposition, numerical approximation .

Research supported in part by U.S. National Science Foundation grant No. DMS-0305080, National Natural Science Foundation of China Project 10228101 and 10301017, and the Basic Research Projects of Tsinghua University under the Project JC2002010.

of width $d\mu$ centered at μ. The function $\sigma(x) > 0$ is the scattering cross-section at position x, while $c(x) > 0$ is the average number of emitted particles per collision at x. Below we assume that $0 < c(x) \leq 1$. When $c = 1$ the material is purely scattering; when $c < 1$ there exist absorbing collisions. The transport equation (1.1) is posed for $x \in (x_{_L}, x_{_R})$ and $\mu \in [-1, 1]$, supplemented with boundary conditions at $x_{_L}$ and $x_{_R}$. Perhaps the simplest example of boundary conditions for (1.1) consists in prescribing the phase-space density of particles entering the domain $(x_{_L}, x_{_R})$ at $x_{_L}$ and $x_{_R}$:

$$\begin{aligned} \Psi(x_{_L}, \mu) &= F_L(\mu)\,, \qquad \text{for } \mu \in (0, 1]\,, \\ \Psi(x_{_R}, -\mu) &= F_R(\mu)\,, \qquad \text{for } \mu \in (0, 1]\,. \end{aligned} \tag{1.2}$$

More general boundary conditions can also be analyzed by the methods of the present paper. For more details on the physical meaning of (1.1)-(1.2), the interested reader is referred to chapter XXI of [7].

Our interest is the numerical computation of (1.1)-(1.2) in the case where the order of magnitude of the scattering cross-section σ varies considerably over the domain $(x_{_L}, x_{_R})$. Such situations are frequently encountered in most applications of transport theory where the background medium is often made of (very) different materials. Specifically, we consider the case of two different materials with an interface located at $x_{_M} \in (x_{_L}, x_{_R})$. At $x_{_M}$, the scattering cross-section σ and emission rate c are assumed to be discontinuous; they are given as follows in terms of a small parameter ϵ:

$$\begin{aligned} &\sigma(x) = 1\,, \qquad \text{and} \quad 0 < c_* \leq c(x) \leq c^* < 1\,, \quad \text{for } x \in (x_{_L}, x_{_M})\,, \\ &\sigma(x) = \epsilon^{-1}\,, \quad \text{and} \quad c(x) = 1 - \epsilon^2 \gamma(x)\,, \qquad \text{for } x \in (x_{_M}, x_{_R})\,. \end{aligned} \tag{1.3}$$

We also make the following assumption (which was used in the mathematical analysis in [13]):

$$0 < \gamma_* \leq \gamma(x) \leq \gamma^*\,, \quad \text{for each } x \in (x_{_M}, x_{_R}) \tag{1.4}$$

for some constants γ_* and γ^*; we shall also restrict our attention to ϵ's such that

$$0 < \epsilon < \epsilon^*\,, \quad \text{where } \epsilon^* < 1/\gamma^*\,. \tag{1.5}$$

Notice that these assumptions exclude the case where c takes the value 1: in particular, the case of a purely scattering, low σ medium is excluded by the assumption (1.3). And when $c = 1$, there will be a counter example to show that the coupling method will not work in section 2.2.4.

The small parameter ϵ is the ratio of the mean free path (the average distance a particle travels between two consecutive collisions with the background medium) to the size of the domain $x_{_R} - x_{_M}$. Changing the space variable x in (1.1) into

$$\begin{aligned} x_{_M} - \int_x^{x_{_M}} \sigma(z)dz \qquad &\text{for } x \in (x_{_L}, x_{_M}) \\ \text{and } x_{_M} + \int_{x_{_M}}^{x} \sigma(z)dz \qquad &\text{for } x \in (x_{_M}, x_{_R}) \end{aligned}$$

one sees that there is no loss of generality in assuming σ to be piecewise constant as in (1.3). (In the context of radiative transfer, the new space variables so defined are referred to as the "optical thickness": see chapter I, §7 in [6].)

Since the mean-free path is small in the region $(x_{_M}, x_{_R})$, we expect that the solution Ψ_ϵ is isotropic (i.e. a function of x alone) to leading order and governed by the diffusion approximation of (1.1). Hence the domain $(x_{_M}, x_{_R})$ is referred to

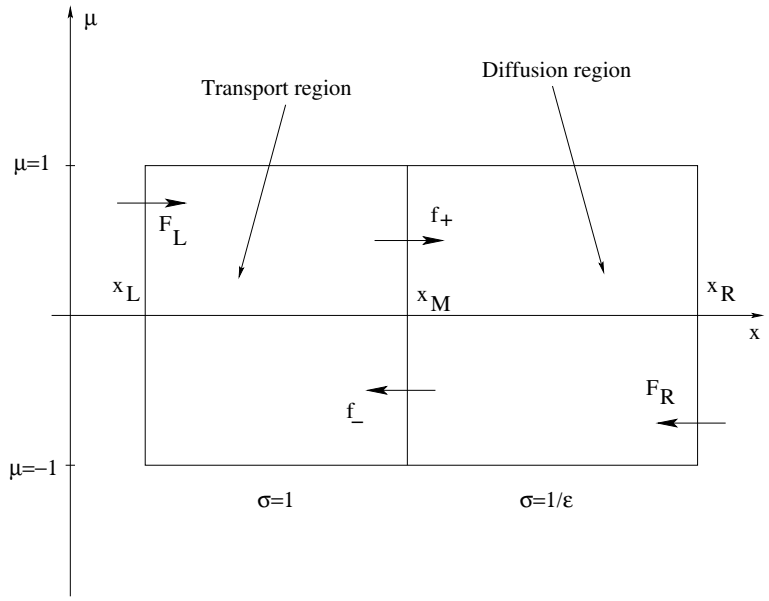

FIGURE 1. Geometry of the one-dimensional interface problem

as "the diffusion region". The smallness of the mean free path in (x_M, x_R) makes it very costly to solve the transport equation accurately there. Solving the diffusion equation on the other hand is much more efficient. By contrast, in the domain (x_L, x_M) one must retain the μ-dependence in the solution Ψ_ϵ and solve the transport equation for Ψ_ϵ in that domain, which will be therefore referred to as "the transport region". For problems like this, it is very natural to use a domain decomposition method which solves the transport equation on the left and the diffusion equation on the right.

Domain decomposition methods matching kinetic and hydrodynamic or diffusion models have received a lot of attention in the past 15 years. Some of the ideas in the present work can be found in [10]; other methods have been proposed in [1], [4], [8], [9], [14], [17], [18], [19], [20], [21], [22], [23]. In the notations of Figure 1, solving the problem (1.1)-(1.2) with coefficients given by (1.3) reduces to finding good approximations of the angle distributions of particles crossing the interface in the direction of the transport domain — i.e. f_- — and in the direction of the diffusive domain — i.e. f_+. In fact, the solution in the diffusive region depends only on some appropriate angle average of f_+, so that the most critical task is to evaluate f_- accurately. In most of the existing domain decomposition methods for this problem — for instance in [1], [23] — this is done by an iteration procedure in which the diffusion and the transport equation are solved alternately until convergence of the successive approximates to f_- and f_+ is reached.

In [13], the authors proposed a boundary condition at x_M on the transport side which mimics the reflection of particles on an infinitely thick, purely scattering domain. This reflection condition is based on almost explicit computations for the steady transport equation in a half-space filled with a purely scattering material. Using this reflection condition yields the correct transport and diffusion solutions in one step up to an $O(\epsilon)$ error and in *two steps* (a prediction-correction algorithm)

up to an $O(\epsilon^2)$ error. In particular, this method *avoids iterating* alternately on the diffusion and transport solutions until convergence of the fluxes at the interface is reached. A complete mathematical justification of the convergence of this method, for the one dimensional case, was done in [13].

In this paper we perform some numerical verification of this domain decomposition method. We conduct numerical experiments for both one and two space dimensions. Our numerical results agree with the convergence analysis of [13]. We also provide an improved second order method that provides more accurate numerical solution than that proposed in [13].

2. The Domain Decomposition Method.

2.1. The reflecting operator and the Chandrasekhar H-function.

The domain decomposition method needs the following two basic quantities for the transport equation. First we define the Chandrasekhar H-function via an integral equation ([6])

$$\frac{1}{H(\mu)} = \int_0^1 \frac{H(\mu')}{2(\mu+\mu')}\mu' d\mu'. \tag{2.1}$$

The density of particles emerging from a purely scattering half-space is

$$(\mathcal{R}G)(\mu) = \frac{1}{2}H(\mu)\int_0^1 G(\mu')\frac{H(\mu')}{\mu+\mu'}\mu' d\mu'. \tag{2.2}$$

The presentation of Chandrasekhar's H-function and of the reflection operator $\mathcal{R}$ arises from [10] pp. 309-311 (in the context of the Boltzmann equation) and is explained explicitly in [11] pp.222-224. Another presentation, according to stochastic processes, can be found in [3].

2.2. The Domain Decomposition Method.

We now review the domain decomposition method proposed in [13].

2.2.1. *Order O(ε) coupling.*

Step 1. Solve the steady transport problem

$$\mu\partial_x\Phi_0 + \Phi_0 - c\overline{\Phi}_0 = 0, \quad (x,\mu)\in(x_L,x_M)\times[-1,1], \tag{2.3}$$

$$\Phi_0(x_L,\mu) = F_L(\mu), \quad \mu\in(0,1], \tag{2.4}$$

$$\Phi_0(x_M,-\mu) = \mathcal{R}(\Phi_0(x_M,\cdot)|_{(0,1]})(\mu), \quad \mu\in(0,1], \tag{2.5}$$

where $\mathcal{R}$ is the reflecting operator defined in (2.2).

Step 2. Using the density Φ_0 provided in Step 1, solve the diffusion problem

$$-\frac{1}{3}\partial_{xx}\Theta_0 + \gamma\Theta_0 = 0, \quad x\in(x_M,x_R), \tag{2.6}$$

$$\Theta_0(x_M) = \frac{\sqrt{3}}{2}\int_0^1 \mu H(\mu)\Phi_0(x_M,\mu)d\mu, \tag{2.7}$$

$$\Theta_0(x_R) = \frac{\sqrt{3}}{2}\int_0^1 \mu H(\mu)\ F_R(\mu)d\mu, \tag{2.8}$$

where H is the Chandrasekhar function defined in (2.1).

The following result was proved in [13].

Theorem 1. *Let Ψ_ε be the solution of the original two-scale steady transport problem (1.1)-(1.2) with coefficients as in (1.3), and define Ψ_0 as follows:*

$$\Psi^0(x,\mu) = \Phi_0(x,\mu), \quad \forall (x,\mu) \in (x_L, x_M) \times [-1,1];$$
$$\Psi^0(x,\mu) = \Theta_0(x), \quad \forall (x,\mu) \in (x_M, x_R) \times [-1,1].$$

Then

$$\|\Psi_\varepsilon - \Phi^0\|_{L^1([x_L,x_R]\times[-1,1])} = O(\varepsilon)$$

and, for each $x'_M, x'_R \in (x_M, x_R)$ such that $x'_M < x'_R$, one has

$$\|\Psi_\varepsilon - \Phi^0\|_{L^2([x_L,x_M]\times[-1,1])} + \|\Psi_\varepsilon - \Phi^0\|_{L^\infty([x'_M,x'_R]\times[-1,1])} = O(\varepsilon)$$

as $\varepsilon \to 0$.

2.2.2. *Order $O(\varepsilon^2)$ coupling.*

In order to obtain a second order scheme, one needs another coupling procedure. At first we solve

$$\mu\partial_x\Phi_1 + \Phi_1 - c\overline{\Phi}_1 = 0, \quad (x,\mu) \in (x_L, x_R) \times [-1,1], \tag{2.9}$$
$$\Phi_1(x_L,\mu) = 0, \quad \mu \in (0,1], \tag{2.10}$$
$$\Phi_1(x_M,-\mu) = \mathcal{R}(\Phi_1(x_M,\cdot)|_{(0,1]})(\mu) + (\lambda+\mu)\partial_x\Theta_0(x_M), \quad \mu \in (0,1]. \tag{2.11}$$

With the results of Φ_1, we continue to compute

$$-\frac{1}{3}\partial_{xx}\Theta_\varepsilon + \gamma\Theta_\varepsilon = 0, \quad x \in (x_M, x_R), \tag{2.12}$$
$$\Theta_\varepsilon(x_M) - \varepsilon\lambda\partial_x\Theta_\varepsilon(x_M) = \frac{\sqrt{3}}{2}\int_0^1 \mu H(\mu)(\Phi_0 + \varepsilon\Phi_1)(x_M,\mu)d\mu, \tag{2.13}$$
$$\Theta_\varepsilon(x_R) + \varepsilon\lambda\partial_x\Theta_\varepsilon(x_R) = \frac{\sqrt{3}}{2}\int_0^1 \mu H(\mu)F_R(\mu)d\mu, \tag{2.14}$$

where λ is given as follows:

$$\lambda = \frac{\sqrt{3}}{2}\int_0^1 \mu^2 H(\mu)d\mu.$$

The following results are from [13].

Theorem 2. *Let Ψ_ε be the solution of the original two-scale steady transport problem (1.1)-(1.2) with coefficients as in (1.3). Define Ψ^1_ε as follows:*

$$\Psi^1_\varepsilon = (\Phi_0 + \varepsilon\Phi_1)(x,\mu), \qquad \forall (x,\mu) \in (x_L, x_M) \times [-1,1];$$

$$\Psi^1_\varepsilon = \Theta_\varepsilon(x) - \varepsilon\mu\partial_x\Theta_\varepsilon(x), \qquad \forall (x,\mu) \in (x_M, x_R) \times [-1,1].$$

Then, for each $x'_M, x'_R \in (x_M, x_R)$ such that $x'_M < x'_R$, one has

$$\|\Psi_\varepsilon - \Psi^1_\varepsilon\|_{L^2([x_L,x_M]\times[-1,1])} + \|\Psi_\varepsilon - \Psi^1_\varepsilon\|_{L^\infty([x'_M,x'_R]\times[-1,1])} = O(\varepsilon^2)$$

as $\varepsilon \to 0$.

2.2.3. *An improved order $O(\varepsilon^2)$ coupling.* Substitute $\partial_x\Theta_0(x_M)$ in (2.9) by $\partial_x\Theta_\varepsilon(x_M)$ derived from (2.12) and compute Ψ_ε^1 again, denoting the result by $\tilde{\Phi}_1$ and $\tilde{\Theta}_\varepsilon$, which satisfies (2.9)-(2.14) with the boundary condition (2.11) changed to

$$\begin{aligned}\tilde{\Phi}_1(x_M,-\mu) &= \mathcal{R}(\tilde{\Phi}_1(x_M,\cdot)|_{(0,1]})(\mu)+(\lambda+\mu)\partial_x\tilde{\Theta}_\varepsilon(x_M), \qquad (2.15)\\ \mu &\in (0,1].\end{aligned}$$

With these definitions, let

$$\tilde{\Psi}_\varepsilon^1 = (\Phi_0+\varepsilon\tilde{\Phi}_1)(x,\mu)x \qquad \forall(x,\mu)\in(x_L,x_M)\times[-1,1]; \qquad (2.16)$$

$$\tilde{\Psi}_\varepsilon^1 = \tilde{\Theta}_\varepsilon(x)-\varepsilon\mu\partial_x\tilde{\Theta}_\varepsilon(x), \qquad \forall(x,\mu)\in(x_M,x_R)\times[-1,1]. \qquad (2.17)$$

Then one gets a similar second order estimate as in Theorem 2 with Ψ_ε^1 replaced by $\tilde{\Psi}_\varepsilon^1$. We call this method the *improved* $O(\varepsilon^2)$ method. Considering that (2.12)-(2.11) are linear equations, we do not need much computation to complete this iteration procedure, i.e. $\tilde{\Phi}_1 = \Phi_1\cdot\dfrac{\partial_x\Theta_\varepsilon}{\partial_x\Theta_0}$, and solving the diffusion equation is a much easier job compared to the transport equation.

Besides, by the procedure which is essentially identical to the proof of Theorem 3.2 in [13] pp. 15-16 (the only difference lies at the expression of function $\psi_\varepsilon(\mu) = \Psi_\varepsilon(x_M,-\mu)-R(\Psi_\varepsilon(x_M,\cdot)|_{(0,1]})(\mu)-(\lambda+\mu)\partial_x\Theta_\varepsilon(x_M))$, the boundary condition derived from (2.15) is a second order one . And because we replace $\partial_x\Theta_0$ with $\partial_x\Theta_\varepsilon$, which leads to the decrease of $\|\psi_\varepsilon\|_{L^\infty}$, the truncation error of this method is expected to be smaller than the original second order method (see [13] pp. 15 (4.28)). This will be confirmed numerically later. And it can also be verified by the fact that Θ_0 is the main value of Θ_ε so that there will be an extra order $O(\varepsilon^2)$ term in order $O(\varepsilon^2)$ coupling than the improved one. Note that the improved $O(\varepsilon^2)$ method is like a prediction-correction method, not an iteration one, which means that to do more iterations is meaningless.

2.2.4. *A counterexample when $c=1$.* Following is another example to show that when $c=1$ the coupling method is not accurate.

Example . We consider one purely scattering problem in one space dimension:

$$\mu\partial_x\Psi(x,\mu)+\sigma(x)\Psi(x,\mu)=\sigma(x)c(x)\overline{\Psi}(x)$$

with isotropic Dirichlet boundary conditions as:

$$\begin{aligned}\Psi(-1,\mu) &= -1-\mu, \quad \text{for } \mu\in(0,1],\\ \Psi(1,-\mu) &= \frac{1}{\varepsilon}-\mu, \quad \text{for } \mu\in(0,1].\end{aligned}$$

It can be easily checked that the analytical true solution is:

$$\begin{aligned}\Psi(x,\mu) &= x-\mu \quad \text{for } x\in[-1,0],\\ \Psi(x,\mu) &= \frac{x}{\varepsilon}-\mu \quad \text{for } x\in(0,1].\end{aligned}$$

While for the $O(\varepsilon)$ coupling method, the solution in the transport domain does not depend on the value of ε, which means the $O(\varepsilon)$ coupling error of the transport domain will not be reduced when ε becomes smaller. So the $O(\varepsilon)$ coupling method is a $O(1)$ one actually.

2.3. **Numerical algorithm.**

2.3.1. *Order O(ε) scheme.* We use the Gauss quadrature to approximate the collision operator. The Gaussian quadrature points of $[0,1]$ are given by μ_m, with the corresponding weight A_m, for $m = 1, \cdots, M$, satisfying

$$\mu_{-m} = -\mu_m, \qquad A_{-m} = A_m.$$

We use the upwind scheme for the transport equation, and center difference for the diffusion equation.
Step 1. In domain $[x_{_L}, x_{_M}]$, setting

$$\begin{aligned} h = \frac{x_M - x_L}{I}, \quad x_i &= x_L + ih, \quad \Phi_i^m = \Phi_0(x_i, \mu_m), \\ i &= 0, \cdots, I, \qquad m = 1, \cdots, M, \end{aligned}$$

then

- For $\mu_m > 0$

$$\frac{\mu_m}{h}(\Phi_i^m - \Phi_{i-1}^m) + \Phi_i^m - \frac{c}{4}\sum_{l=-M}^{M} A_l \Phi_i^l = 0;$$

- for $\mu_{-m} < 0$

$$\frac{\mu_{-m}}{h}(\Phi_{i+1}^{-m} - \Phi_i^{-m}) + \Phi_i^{-m} - \frac{c}{4}\sum_{l=-M}^{M} A_l \Phi_i^l = 0.$$

- Using the Gauss quadrature again, we obtain the discrete boundary conditions

$$\Phi_0^m = F_L(\mu_m), \quad m = 1, \cdots, M,$$

$$\Phi_I^{-m} = \frac{1}{4} H(\mu_m) \sum_{l=1}^{M} \frac{\mu_l H(\mu_l)}{\mu_m + \mu_l} A_l \Phi_I^l.$$

Step 2. In domain $[x_{_M}, x_{_R}]$, setting

$$h = \frac{x_R - x_M}{J}, \quad x_j = x_M + jh, \qquad j = 0, \cdots, J, \quad \Theta_j = \Theta_0(x_j),$$

we use

$$-\frac{1}{3}\frac{\Theta_{j+1} - 2\Theta_j + \Theta_{j-1}}{h^2} + \gamma\Theta_j = 0, \tag{2.18}$$

with the boundary condition

$$\Theta_0 = \frac{\sqrt{3}}{4}\sum_{l=1}^{M} \mu_l H(\mu_l) A_l \Phi_I^l,$$

$$\Theta_J = \frac{\sqrt{3}}{4}\sum_{l=1}^{M} \mu_l H(\mu_l) A_l F_R(\mu_l).$$

2.3.2. *Order $O(\varepsilon^2)$ scheme.*

Step 1. Observing that (2.9) differs from (2.3) only in the right hand side of the equations, so one just needs a discretization of $\partial_x\Theta_0(x_{_M})$, and we use the second order formula

$$\partial_x\Theta_0(x_{_M}) = \frac{-\Theta_0(x_{_M}+2h)+4\Theta_0(x_{_M}+h)-3\Theta_0(x_{_M})}{h}+O(h^2).$$

Step 2. We use fictitious points to discretize the diffusion boundary conditions in order to gain a second order accuracy in the diffusion region (to be the same order of accuracy as the interior of the domain $[x_{_M}, x_{_R}]$). Using

$$\partial_x\Theta_\varepsilon(x_{_M}) = \frac{\Theta_1-\Theta_{-1}}{2h}+O(h^2),$$

then the left boundary condition is discretized as

$$\Theta_0-\varepsilon\lambda\frac{\Theta_1-\Theta_{-1}}{2h} = \frac{\sqrt{3}}{2}\int_0^1 \mu H(\mu)(\Phi_0+\varepsilon\Phi_1)(x_{_M},\mu)d\mu.$$

Using (2.12) at $x_{_M}$,

$$-\frac{1}{3}\frac{\Theta_1-2\Theta_0+\Theta_{-1}}{h^2}+\gamma\Theta_0 = 0.$$

By combining these two equations, one gets the second order approximation of the diffusion boundary condition at $x_{_M}$:

$$-\frac{\varepsilon\lambda}{h}\Theta_1+\left(1+\frac{3h}{2}\varepsilon\lambda(\frac{2}{3h^2}+\gamma)\right)\Theta_0 = \frac{\sqrt{3}}{4}\sum_{l=1}^{M}\mu_l H(\mu_l)(\Phi_0+\varepsilon\Phi_1)(x_{_M},\mu_l).$$

Similarly, the diffusion boundary condition at $x_{_R}$ is discretized by

$$\left(1+\frac{3h}{2}\varepsilon\lambda(\frac{2}{3h^2}+\gamma)\right)\Theta_J-\frac{\varepsilon\lambda}{h}\Theta_{J-1} = \frac{\sqrt{3}}{4}\sum_{l=1}^{M}\mu H(\mu_l)F_R(\mu_l).$$

In the interior of the domain, the same second order centered difference scheme as in (2.18).

Step 3. Replacing the (discrete) $\partial_x\Theta_0(x_{_M})$ of step 1 with $\partial_x\Theta_\varepsilon(x_{_M})$ of step 2, we obtain the numerical approximation of $\tilde{\Psi}^1_\varepsilon$.

3. **Two Dimensional Case.**

3.1. **The Problem.** We first introduce the two-dimensional transport equation with two spatial scales. Consider the two-dimensional transport equation:

$$\omega\cdot\nabla_x\Psi(x,\omega)+\sigma(x)\Psi(x,\omega) = \sigma(x)c(x)\overline{\Psi}(x), \tag{3.1}$$

$$\text{where}\quad \overline{\Psi}(x) = \frac{1}{|\mathbf{S}^{D-1}|}\int_{\mathbf{S}^{D-1}}\Psi(x,\omega)d\omega, \tag{3.2}$$

with boundary condition

$$\Psi(x,\omega) = F_b(x,\omega),\qquad for\ \ (x,\omega)\in\Sigma^-. \tag{3.3}$$

where

$$\Sigma^- = \{(x,\omega)\in\partial\Omega\times\mathbf{S}^{D-1}|\omega\cdot n_x<0\} \tag{3.4}$$

and n_x is an unit outward normal of $\partial\Omega$ locating at the point x.

The transport coefficients are assumed to be scaled as:

$$\sigma = \sigma_T(x), \quad \text{and} \quad c(x) = c_T(x) \in (0,1), \quad \text{for} \ \ x \in \Omega_T, \tag{3.5}$$

$$\sigma(x) = \varepsilon^{-1}\sigma_D(x), \quad \text{and} \quad c(x) = 1 - \varepsilon^2\gamma(x), \quad \text{for} \ \ x \in \Omega_D, \tag{3.6}$$

where the physical meaning of $c(x), \sigma(x), \varepsilon$ is the same as the one-dimensional model, while ω expresses the direction of the particles, which is therefore similar to the variable μ. Functions $\sigma_T(x)$,$\sigma_D(x)$,$\gamma(x)$ are assumed to be smooth with $\sigma(x) > 0$ and $c(x) > 0$.

Assume Ω is a convex domain with smooth boundary, and Ω_D representing the diffusion region is also a similar one while its closure $\overline{\Omega}_D$ is included in Ω . $\Omega_T = \Omega \setminus \Omega_D$ is the transport region (see figure 2).

3.2. **The H-Function and the Reflecting Operator.** Let $\mathbf{S}_\nu^- = \{\omega \in \mathbf{S}^{D-1} | \omega \cdot \nu < 0\}$ and denote the reflection with the respect to ω by $s_\nu(\omega) = \omega - 2(\omega \cdot \nu)\nu$. Then the multidimensional H-function is defined by

$$\frac{1}{H_\nu(\omega)} = \frac{1}{|\mathbf{S}^{D-1}|} \int_{\mathbf{S}_\nu^-} \frac{H_\nu(\omega')}{|\omega \cdot \nu| + |\omega' \cdot \nu|} \, |\omega' \cdot \nu| \, d\omega', \tag{3.7}$$

while the reflecting operator is given by

$$\mathcal{R}_\nu G(\omega) = \frac{1}{|\mathbf{S}^{D-1}|} \int_{\mathbf{S}_\nu^-} r_\nu(\omega, \omega') G(\omega') \, |\omega' \cdot \nu| \, d\omega'. \tag{3.8}$$

For the diffusion boundary conditions we also need

$$\Lambda_\nu(G) = \frac{1}{K \cdot |\mathbf{S}^{D-1}|} \int_{\mathbf{S}_\nu^-} |\omega \cdot \nu| \, G(\omega) H_\nu(\omega) d\omega \tag{3.9}$$

with r and K defined as

$$r_\nu(\omega, \omega') = \frac{H_\nu(\omega) H_\nu(\omega')}{|\omega \cdot \nu| + |\omega' \cdot \nu|} \text{ and } K = \sqrt{\frac{1}{|\mathbf{S}^{D-1}|} \int_{\mathbf{S}^{D-1}} (\omega \cdot \nu)^2 d\omega}.$$

The equation (3.7) suggests that H_ν only depends on $\omega \cdot \nu$, then with the notation

$$H_\nu(\omega) = \mathcal{H}_D(|\omega \cdot \nu|)$$

one will get

$$\frac{1}{\mathcal{H}_D(\mu)} = \frac{|\mathbf{S}^{D-2}|}{|\mathbf{S}^{D-1}|} \int_0^1 \frac{\mathcal{H}_D(\mu')}{\mu + \mu'} \mu' (1 - \mu'^2)^{\frac{D-3}{2}} d\mu' \tag{3.10}$$

which is a analogous to the one-dimensional definition in (2.1).

3.3. **A Domain Decomposition Method.** In terms of the function Λ_ν and the reflection operator $\mathcal{R}_\nu$, an $O(\varepsilon)$ algorithm was given in [13] as follows:

Given the notations

$$\begin{aligned} \Sigma_i^+ = \ & \{(x, \omega) \in \partial\Omega_D \times \mathbf{S}^{D-1} | \omega \cdot \nu_x > 0\} \\ \Sigma_i^- = \ & \{(x, \omega) \in \partial\Omega_D \times \mathbf{S}^{D-1} | \omega \cdot \nu_x < 0\} \end{aligned} \tag{3.11}$$

where γ_x is the outward normal to Ω_D at the point $x \in \partial\Omega_D$.

- on the transport domain Ω_T, solve

$$\begin{aligned} \omega \cdot \nabla_x \Phi(x, \omega) + \sigma(x)\Phi(x, \omega) &= \sigma(x) c(x) \overline{\Phi}(x), \ \text{for} \ \ (x, \omega) \in \Omega_T \times \mathbf{S}^{D-1}, \\ \Phi(x, \omega) &= F_b(x, \omega), \qquad \text{for} \ \ (x, \omega) \in \Sigma^-, \\ \Phi(x, s_{\nu_x}(x)) &= \mathcal{R}_{\nu_x} \Phi(x, \omega), \quad \text{for} \ \ (x, \omega) \in \Sigma_i^-. \end{aligned} \tag{3.12}$$

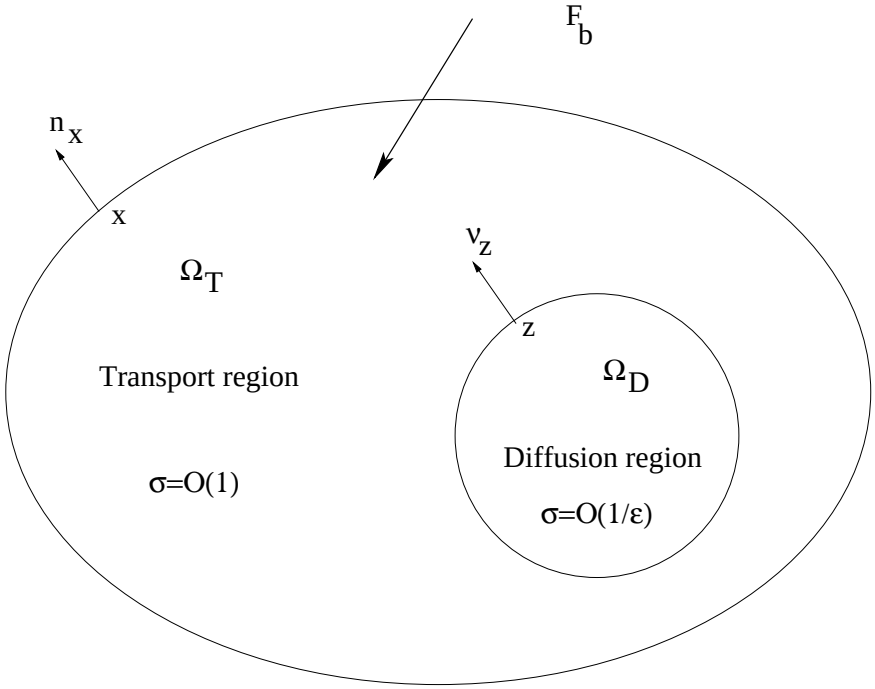

FIGURE 2. Geometry of the multi-dimensional interface problem

- on the diffusion domain Ω_D, solve

$$\begin{aligned} \gamma\Theta(x) - \frac{1}{D}\nabla_x \cdot \left(\frac{1}{\sigma(x)\nabla_x\Theta(x)}\right) &= 0, \qquad && \text{on} \quad \Omega_D, \\ \Theta(x) &= \Lambda_{\nu_x}(\Phi(x,\cdot)), && \text{on} \quad \partial\Omega_T, \end{aligned} \tag{3.13}$$

  where $\mathcal{R}_{\nu_x}$ and Λ_{ν_x} are expressed in (3.8) and (3.9) respectively.

The following theorem, proved in [13], gives an error estimate of this coupling scheme.

Theorem 3. *Let Ψ_ε be the solution of the original high-dimensional problem (3.1)-(3.5) with parameters described as in (3.3), define Ψ^2 as follows:*

$$\begin{aligned} \Psi^2(x,\omega) &= \Phi(x,\omega), \qquad if \quad x \in \Omega_T; \\ \Psi^2(x,\omega) &= \Theta(x), \qquad if \quad x \in \Omega_D. \end{aligned}$$

Then

$$\left\|\Psi_\varepsilon - \Psi^2\right\|_{L^1(\Omega\times\mathbf{S}^{D-1})} = O(\varepsilon)$$

and for any smooth convex domain Ω'_D satisfying $\overline{\Omega'_D} \subset \Omega_D$, one has

$$\left\|\Psi_\varepsilon - \Psi^2\right\|_{L^2(\Omega_T\times\mathbf{S}^{D-1})} + \left\|\Psi_\varepsilon - \Psi^2\right\|_{L^\infty(\Omega'_D\times\mathbf{S}^{D-1})} = O(\varepsilon) \tag{3.14}$$

as $\varepsilon \to 0$.

3.4. **Numerical algorithm.** We now describe our numerical discretization in the cases where both Ω and Ω_D are rectangles in $\mathbf{R}^2$. We smooth out the corners to avoid singularities.

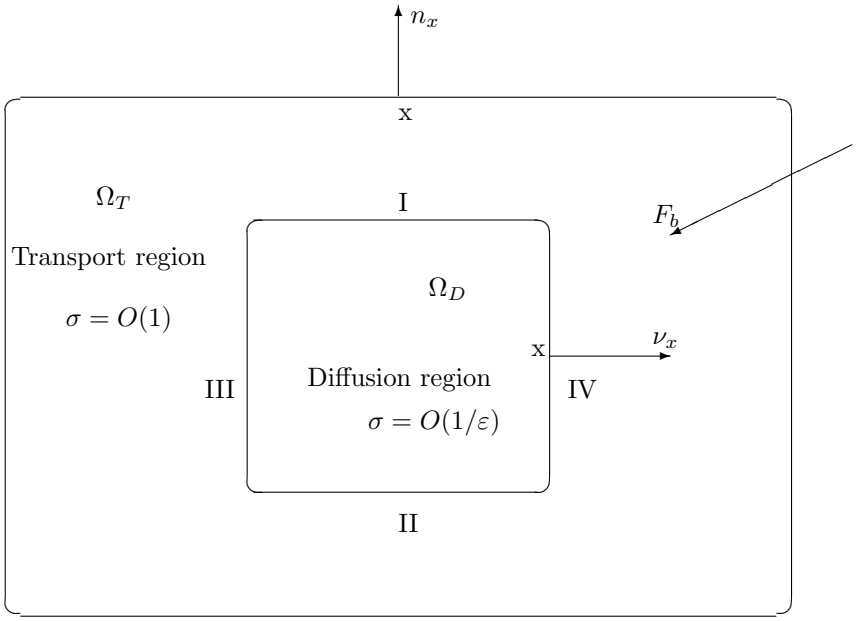

Figure 3. The interface problem of high dimensions

Suppose $\Omega = [x_L, x_R] \times [y_D, y_U]$. Define the discrete direction vector as

$$\begin{aligned} \omega_1^m &= (\sqrt{1-\alpha_m^2}, \alpha_m), \qquad \omega_2^m = (-\sqrt{1-\alpha_m^2}, \alpha_m), \\ \omega_3^m &= (-\sqrt{1-\alpha_m^2}, -\alpha_m), \qquad \omega_4^m = (\sqrt{1-\alpha_m^2}, -\alpha_m), \end{aligned}$$

where $\alpha_m = \sin(\frac{\pi}{2}\mu_m)$, μ_m being the one-dimensional Gaussian quadrature points over $[0,1]$, with weight A_m. We divide the interface $\partial\Omega_D$ into four parts I, II, III, and IV with unit normals ν_1, ν_2, ν_3, and ν_4 respectively (see figure 3).

Step 1. In the domain Ω_T. Let

$$\begin{aligned} x_i &= x_L + ih, \quad i = 0, \cdots, I, \quad y_j = y_D + jh, \quad j = 0, \cdots, J, \\ h &= \frac{x_R - x_L}{I} = \frac{y_U - y_D}{J}, \qquad \Phi_{ijk}^m = \Phi(x_i, y_j, \omega_k^m), \\ m &= 1, \cdots, M, \qquad k = 1, \cdots, 4. \end{aligned} \tag{3.15}$$

The discretization the transport equation is done by the upwind scheme:

- in the first quadrant of ω-plane:

$$\begin{aligned} &\sqrt{1-\alpha_m^2}\frac{\Phi_{ij1}^m - \Phi_{i-1,j1}^m}{h} + \alpha_m \frac{\Phi_{ij1}^m - \Phi_{i,j-1,1}^m}{h} + \sigma_{ij}\Phi_{ij1}^m \\ &= \frac{1}{8}\sigma_{ij}c_{ij}\sum_{l=1}^{M}\sum_{k=1}^{4} A_l \Phi_{ijk}^l; \end{aligned}$$

- in the second quadrant of ω-plane:

$$
\begin{aligned}
&-\sqrt{1-\alpha_m^2}\frac{\Phi^m_{i,j+1,1}-\Phi^m_{ij1}}{h}+\alpha_m\frac{\Phi^m_{ij1}-\Phi^m_{i,j-1,1}}{h}+\sigma_{ij}\Phi^m_{ij1}\\
&=\frac{1}{8}\sigma_{ij}c_{ij}\sum_{l=1}^{M}\sum_{k=1}^{4}A_l\Phi^l_{ijk};
\end{aligned}
$$

- in the third quadrant of ω-plane:

$$
\begin{aligned}
&-\sqrt{1-\alpha_m^2}\frac{\Phi^m_{i,j+1,1}-\Phi^m_{ij1}}{h}-\alpha_m\frac{\Phi^m_{i,j+1,1}-\Phi^m_{ij1}}{h}+\sigma_{ij}\Phi^m_{ij1}\\
&=\frac{1}{8}\sigma_{ij}c_{ij}\sum_{l=1}^{M}\sum_{k=1}^{4}A_l\Phi^l_{ijk};
\end{aligned}
$$

- in the fourth quadrant of ω-plane:

$$
\begin{aligned}
&\sqrt{1-\alpha_m^2}\frac{\Phi^m_{ij1}-\Phi^m_{i-1,j1}}{h}-\alpha_m\frac{\Phi^m_{i,j+1,1}-\Phi^m_{ij1}}{h}+\sigma_{ij}\Phi^m_{ij1}\\
&=\frac{1}{8}\sigma_{ij}c_{ij}\sum_{l=1}^{M}\sum_{k=1}^{4}A_l\Phi^l_{ijk}.
\end{aligned}
$$

The numerical boundary conditions at the interfaces $\partial\Omega_D$ are:

- the top boundary I:

$$
\Phi^m_{ij1}=\Phi^m_{ij2}=\frac{1}{8}\sum_{k=3,4}\sum_{l=1}^{M}\frac{\left|\omega^l_k\cdot\nu_1\right|A_lH(\left|\omega^l_k\cdot\nu_1\right|)}{\left|\omega^l_k\cdot\nu_1\right|+\left|\omega^m_k\cdot\nu_1\right|}\Phi^l_{ijk}H(|\omega^m_k\cdot\nu_1|);
$$

- the bottom boundary II:

$$
\Phi^m_{ij3}=\Phi^m_{ij4}=\frac{1}{8}\sum_{k=1,2}\sum_{l=1}^{M}\frac{\left|\omega^l_k\cdot\nu_2\right|A_lH(\left|\omega^l_k\cdot\nu_2\right|)}{\left|\omega^l_k\cdot\nu_2\right|+\left|\omega^m_k\cdot\nu_2\right|}\Phi^l_{ijk}H(|\omega^m_k\cdot\nu_2|);
$$

- the left boundary III:

$$
\Phi^m_{ij2}=\Phi^m_{ij3}=\frac{1}{8}\sum_{k=1,4}\sum_{l=1}^{M}\frac{\left|\omega^l_k\cdot\nu_3\right|A_lH(\left|\omega^l_k\cdot\nu_3\right|)}{\left|\omega^l_k\cdot\nu_3\right|+\left|\omega^m_k\cdot\nu_3\right|}\Phi^l_{ijk}H(|\omega^m_k\cdot\nu_3|);
$$

- the right boundary IV:

$$
\Phi^m_{ij1}=\Phi^m_{ij4}=\frac{1}{8}\sum_{k=2,3}\sum_{l=1}^{M}\frac{\left|\omega^l_k\cdot\nu_4\right|A_lH(\left|\omega^l_k\cdot\nu_4\right|)}{\left|\omega^l_k\cdot\nu_4\right|+\left|\omega^m_k\cdot\nu_4\right|}\Phi^l_{ijk}H(|\omega^m_k\cdot\nu_4|).
$$

Step 2. In domain Ω_D, let

$$
x_i=x_L+ih,\quad i=0,\cdots,L,\qquad y_j=y_D+jh,\quad j=0,\cdots,n,
$$

$$
h=\frac{x_R-x_L}{L}=\frac{y_U-y_D}{N},\qquad \Theta_{ij}=\overline{\Psi}(x_i,y_j).
$$

Applying the centered difference scheme will result in:

$$\gamma_{ij}\Theta_{ij} - \frac{1}{D}\left[\frac{\frac{1}{\sigma_{i+1/2,j}}(\Theta_{i+1,j}-\Theta_{ij}) - \frac{1}{\sigma_{i-1/2,j}}(\Theta_{ij}-\Theta_{i-1,j})}{h^2} - \frac{\frac{1}{\sigma_{i,j+1/2}}(\Theta_{i,j+1}-\Theta_{ij}) - \frac{1}{\sigma_{i,j-1/2}}(\Theta_{ij}-\Theta_{i,j-1})}{h^2}\right] = 0,$$

where

$$\sigma_{i+\frac{1}{2},j} = \sigma(\frac{1}{2}(x_j + x_{j+1}), y_j), \qquad \sigma_{i-\frac{1}{2},j} = \sigma(\frac{1}{2}(x_{j-1} + x_j), y_j)$$

$$\sigma_{i,j+\frac{1}{2}} = \sigma(x_j, \frac{1}{2}(y_j + y_{j+1})), \qquad \sigma_{i,j-\frac{1}{2}} = \sigma(x_j, \frac{1}{2}(y_{j-1} + y_j))$$

The boundary conditions at $\partial\Omega_D$ are the discretization of (3.9) by the Gauss quadrature:

- the top boundary I:

$$\Theta_{ij} = \frac{1}{2K\cdot|\mathbf{S^{D-1}}|}\sum_{k=3,4}\sum_{l=1}^{M}\left|\omega_k^l\cdot\nu_1\right| A_l H(\left|\omega_k^l\cdot\nu_1\right|)\Phi_{ijk}^l;$$

- the bottom boundary II:

$$\Theta_{ij} = \frac{1}{2K\cdot|\mathbf{S^{D-1}}|}\sum_{k=1,2}\sum_{l=1}^{M}\left|\omega_k^l\cdot\nu_2\right| A_l H(\left|\omega_k^l\cdot\nu_2\right|)\Phi_{ijk}^l;$$

- the left boundary III:

$$\Theta_{ij} = \frac{1}{2K\cdot|\mathbf{S^{D-1}}|}\sum_{k=1,4}\sum_{l=1}^{M}\left|\omega_k^l\cdot\nu_3\right| A_l H(\left|\omega_k^l\cdot\nu_3\right|)\Phi_{ijk}^l;$$

- the right boundary IV:

$$\Theta_{i,j} = \frac{1}{2K\cdot|\mathbf{S^{D-1}}|}\sum_{k=2,3}\sum_{l=1}^{M}\left|\omega_k^l\cdot\nu_4\right| A_l H(\left|\omega_k^l\cdot\nu_4\right|)\Phi_{ijk}^l.$$

4. **Numerical examples.** We give three numerical examples, two in one space dimension and one in two space dimension. As a comparison we also solve the transport equation in the entire domain by the same method as in the domain decomposition method (namely upwind for space derivative and Gauss quadrature for the collision operator), with space cells much smaller than ε.

Example 1. First, we consider a purely scattering problem in one space dimension:

$$\mu\,\partial\Psi(x,\mu) + \sigma(x)\Psi(x,\mu) = \sigma(x)c(x)\overline{\Psi}(x)$$

where

$$\sigma = 1, \quad \text{and} \quad c = 1, \quad \text{for } x\in(-1,0),$$

$$\sigma = \frac{1}{\varepsilon}, \quad \text{and} \quad c = 1, \quad \text{for } x\in(0,1),$$

with isotropic Dirichlet boundary conditions as:

$$\Psi(-1,\mu) = 1, \quad \text{for } \mu\in(0,1],$$

$$\Psi(1,-\mu) = 2, \quad \text{for } \mu\in(0,1],$$

which shows that $\gamma = 0$ by (1.3).

We take $h = 1.0E-5$ for the true solution and transport domain solution and $h = 1.0E-4$ for the diffusion domain. The results of $\varepsilon = 0.1$ based on the $O(\varepsilon)$, $O(\varepsilon^2)$ and the improved $O(\varepsilon^2)$ methods are shown in figures 4. Error estimating forms with different ε values are shown in Table 1-3. From the error tables, one can see that although the coupling methods are not accurate at the case of $c = 1$, however, we still can get an good approximation solution through the improved $O(\varepsilon^2)$ coupling method in this example, that also shows its powerful efficiency.

Example 2. This is a one-dimensional example with small absorption ($c < 1$). Suppose that $\gamma = 1$. The coefficients and outer boundary conditions are given by

$$\begin{aligned} &\sigma = 1, \quad \text{and} \quad c = 0.9, \quad \text{for } x \in (-1, 0), \\ &\sigma = 10, \quad \text{and} \quad c = 1 - \varepsilon^2\gamma, \quad \text{for } x \in (0, 1); \end{aligned}$$

$$\begin{aligned} \Psi(-1, \mu) &= 1, \quad \text{for } \mu \in (0, 1], \\ \Psi(1, -\mu) &= 1, \quad \text{for } \mu \in (0, 1]. \end{aligned}$$

The numerical results for $\varepsilon = 0.1$ using $h = 1.0E-5$ in transport domain and $h = 1E-4$ in diffusion domain are shown in figure 5, in which the true solution is obtained by taking $h = 1.0E-5$ with the upwind scheme for the whole two-scale transport problem. The desired accuracy in ε is observed, with remarkably accurate results for the improved $O(\varepsilon^2)$ solution. Besides, for $\varepsilon = 0.20$ and 0.05 after taking the same steps, we also get some good results. Error estimating forms with different ε values are shown in Table 4-6, which confirm the conclusions of Theorem 1 and Theorem 2. Table 4 also shows that the difference between $\partial\Theta_\varepsilon$ and $\partial\Theta_0$ is really an order $O(\varepsilon)$ term, which provides us with the evidence that the improved coupling method is a real second order one. Besides, Table 5 not only confirms that the improved coupling method is an order $O(\varepsilon^2)$ algorithm, but also verifies that the truncation error has been greatly reduced by the improved coupling. And at the same time we also compute another norm to estimate the errors of coupling methods, see Table 6. From Table 6 one may say that the improved method is slightly better than the old second order method. That is because what the new $O(\varepsilon^2)$ coupling method improves is a first order revision to the $\partial_x\Theta_\varepsilon$, which improves much of the transport solution, while for the boundary layer (when ε is small) near x_M which offers most parts of the L^∞ norm error, it will contribute less. So if we use the L^∞ norm in $[x'_M, x'_R]$ of the diffusion domain, the difference of the errors between the old and new $O(\varepsilon^2)$ coupling methods will be slight, while if using L^2 norm, the difference will be large (see Table 5). Following is a two-dimensional problem example. To show the efficiency of the domain decomposition methods clearly, we choose $\varepsilon = 0.1$.

Example 3. This is a two-dimensional problem defined in $\Omega = [-0.5, 0.5] \times [-0.5, 0.5]$, with $\Omega_D = [-0.25, 0.25] \times [-0.25, 0.25]$. In this case, $D = 2$, $K = \frac{\sqrt{2}}{2}$. Suppose $F_b(x, \omega) = 1$, $\varepsilon = 0.1$ and $\gamma = 1$. The problem to be solved is

$$\omega \cdot \nabla_x \Psi(x, \omega) + \sigma(x)\Psi(x, \omega) = \sigma(x)c(x)\overline{\Psi}(x),$$

ε	$\|\Psi_\varepsilon - \Phi^0\|_1$	$\|\partial_x\Theta_\varepsilon(x_M) - \partial_x\Theta_0(x_M)\|$
0.20	5.408E-1	3.826E-1
0.10	3.234E-1	2.151E-1
0.05	1.794E-1	1.147E-1

TABLE 1. $\|\cdot\|_1 = \|\cdot\|_{L^1([x_L,x_R]\times[-1,1])}$.

ε	$\|\Psi_\varepsilon - \Phi^0\|_2$	$\|\Psi_\varepsilon - \Psi^1_\varepsilon\|_2$	$\|\Psi_\varepsilon - \tilde{\Psi}^1_\varepsilon\|_2$
0.20	4.089E-1	1.927E-1	2.046E-2
0.10	2.444E-1	6.174E-2	4.240E-3
0.05	1.339E-1	1.917E-2	3.599E-3

TABLE 2. $\|\cdot\|_2 = \|\cdot\|_{L^2([x_L,x_M]\times[-1,1])} + \|\cdot\|_{L^2([x'_M,x'_R]\times[-1,1])}$.

ε	$\|\Psi_\varepsilon - \Phi^0\|_3$	$\|\Psi_\varepsilon - \Psi^1_\varepsilon\|_3$	$\|\Psi_\varepsilon - \tilde{\Psi}^1_\varepsilon\|_3$
0.20	6.884E-1	2.608E-1	1.105E-1
0.10	4.113E-1	1.102E-1	5.576E-2
0.05	2.258E-1	4.807E-2	3.387E-2

TABLE 3. $\|\cdot\|_3 = \|\cdot\|_{L^2([x_L,x_M]\times[-1,1])} + \|\cdot\|_{L^\infty([x'_M,x'_R]\times[-1,1])}$.

ε	$\|\Psi_\varepsilon - \Phi^0\|_1$	$\|\partial_x\Theta_\varepsilon(x_M) - \partial_x\Theta_0(x_M)\|$
0.20	4.650E-1	2.179E-1
0.10	2.580E-2	1.179E-1
0.05	1.366E-2	6.151E-2

TABLE 4. $\|\cdot\|_1 = \|\cdot\|_{L^1([x_L,x_R]\times[-1,1])}$.

with

$$\begin{aligned} \sigma &= 1, \quad \text{and} \quad c = 0.9, \quad \text{for} \quad x \in \Omega_T, \\ \sigma &= 10, \quad \text{and} \quad c = 0.99, \quad \text{for} \quad x \in \Omega_D. \end{aligned}$$

The numerical results the of $O(\varepsilon)$ method using $h = 0.01$ are given in figures 6-8.

ε	$\|\Psi_\varepsilon - \Phi^0\|_2$	$\|\Psi_\varepsilon - \Psi^1_\varepsilon\|_2$	$\|\Psi_\varepsilon - \tilde{\Psi}^1_\varepsilon\|_2$
0.20	3.369E-1	8.228E-2	4.020E-2
0.10	1.862E-1	2.587E-2	1.285E-2
0.05	9.827E-2	8.239E-3	4.371E-3

TABLE 5. $\|\cdot\|_2 = \|\cdot\|_{L^2([x_L,x_M]\times[-1,1])} + \|\cdot\|_{L^2([x'_M,x'_R]\times[-1,1])}$.

ε	$\|\Psi_\varepsilon - \Phi^0\|_3$	$\|\Psi_\varepsilon - \Psi^1_\varepsilon\|_3$	$\|\Psi_\varepsilon - \tilde{\Psi}^1_\varepsilon\|_3$
0.20	5.453E-1	2.375E-1	1.706E-1
0.10	3.112E-1	1.111E-1	8.952E-2
0.05	1.673E-1	5.303E-2	4.725E-2

TABLE 6. $\|\cdot\|_3 = \|\cdot\|_{L^2([x_L,x_M]\times[-1,1])} + \|\cdot\|_{L^\infty([x'_M,x'_R]\times[-1,1])}$.

5. Appendix A: Tabulate H-function.

Using the Gauss quadrature,

$$\int_{-1}^{1} f(x)dx = \sum_{k=1}^{M} A_k f(\mu_k) + R_n[f], \tag{5.1}$$

equation (2.1) can be discretized as

$$\frac{1}{H(\mu_k)} = \frac{1}{4}\sum_{l=1}^{M} \frac{\mu_l H(\mu_l)}{\mu_k + \mu_l} A_l\,, \quad k = 1, \cdots, M,$$

where μ_k are the Gaussian quadrature points over $[0,1]$ with the corresponding weight A_k.

Setting $H(\mu_k) = X_k$ leads to

$$\frac{1}{4}\sum_{l=1}^{N} \frac{\mu_l A_l X_k X_l}{\mu_k + \mu_l} - 1 = 0. \tag{5.2}$$

By letting $X = (X_1, \cdots, X_N)^T$ and $F(X) = (F_1(X), \cdots, F_N(X))^T$, one can use the Newton Iteration to tabulate the H-function:

$$X^{k+1} = X^k - D^{-1}F(X^k)\cdot F(x^k), \tag{5.3}$$

where

$$F_k(X) = \frac{1}{4}\sum_{l=1}^{N} \frac{\mu_l A_l X_k \cdot X_l}{\mu_k + \mu_l} - 1 = 0,$$

and $DF(X) = \left(\frac{\partial F}{\partial X_1}, \frac{\partial F}{\partial X_2}, \cdots, \frac{\partial F}{\partial X_N}\right) =$

$$\frac{1}{4}\begin{pmatrix} A_1X_1 + \sum_{l\neq 1}\frac{\mu_l A_l X_l}{\mu_1+\mu_l} & \frac{\mu_2 A_2 X_1}{\mu_1+\mu_2} & \cdots & \cdots & \frac{\mu_n A_n X_1}{\mu_1+\mu_N} \\ \frac{\mu_1 A_1 X_2}{\mu_2+\mu_1} & A_2X_2 + \sum_{l\neq 2}\frac{\mu_l A_l X_l}{\mu_2+\mu_l} & \frac{\mu_3 A_3 X_3}{\mu_2+\mu_3} & \cdots & \frac{\mu_n A_n X_2}{\mu_2+\mu_N} \\ \vdots & \ddots & \ddots & \ddots & \vdots \\ \vdots & \ddots & \ddots & \ddots & \vdots \\ \vdots & \ddots & \ddots & \ddots & \vdots \\ \vdots & \ddots & \ddots & \ddots & \vdots \end{pmatrix}$$

The graph of H-function is on figure 9, and the discrete values of one-dimensional problem are listed in table 7. By almost the same way, we obtain the graph of H in the two-dimensional problem (see the figure 10 and table 8).

u_k	X_k
0.01985507175	1.06140994454730
0.10166676130	1.25088788493250
0.23723379505	1.52276222262328
0.40828267875	1.84458076013795
0.59171732125	2.17917814046071
0.76276620495	2.48626918656969
0.89833323870	2.72763016718132
0.98014492825	2.87266987430492

TABLE 7. The values of H-function in one-dimensional problem, M=8

$\lvert\omega^k \cdot \nu\rvert$	X_k
0.03118321783	1.06836148422777
0.15901983478	1.28797460262252
0.36408107700	1.60433394553000
0.59826084448	1.95114484085644
0.80130141766	2.24679274859548
0.93136725805	2.43482245820158
0.98727538820	2.51541359436124
0.99951368521	2.53303903557824

TABLE 8. The values of H-function in two-dimensional problem, M=8

6. **Appendix B: The Reflector For The General Linear Transport Equation.** The following is about the reflector of the general linear transport equation,

$$\omega \cdot \nabla \Psi(x,\omega) + \Sigma(x)\Psi(x,\omega) = \tilde{K}\Psi(x,\omega) + q(x), \quad in \quad \Omega \times W,$$

where

$$\tilde{K}\Psi(x,\omega) = \sigma_s(x) \int_W f(\omega',\omega)\Psi(x,\omega')d\mu(\omega').$$

and

$$\int_W f(\omega',\omega)d\mu(\omega') = 1$$

After changing variables to lengthen the boundary layer and ignoring the $O(\varepsilon^2)$ terms, we have the half-space transport problem:

$$\begin{aligned} -(\omega\cdot\nu)\partial_z\Gamma(z,\omega) + \Gamma(z,\omega) - \overline{\Gamma}(z,\omega) = 0, \\ \Gamma(0,\omega) = G(\omega), \qquad \omega\cdot\nu < 0, \end{aligned} \tag{6.4}$$

where

$$\overline{\Gamma}(x,\omega) = \frac{1}{|\mathbf{S}^{D-1}|}\int_{\mathbf{S}^{D-1}} f(\omega',\omega)\Gamma(x,\omega')d\omega'$$

In addition, there exists a linear functional Λ_ν and a bounded operator $\mathcal{R}_\nu$ both acting on $L^2(\mathbf{S}^-_\nu, |\omega\cdot\nu|d\omega)$ such that

$$\begin{aligned} \Gamma(z,\omega) \to \Gamma_\infty = \Lambda_\nu(G) \text{ for each } \omega \in \mathbf{S}^{D-1} \text{ and} \\ \Gamma(0,\mathbf{s}_\nu(\omega)) = (\mathcal{R}_\nu G)(\omega) \text{ for each } \omega \in \mathbf{S}^-_\nu, \end{aligned} \tag{6.5}$$

with the notation $\mathbf{s}_\nu(\omega) = \omega - 2(\omega\cdot\nu)\nu$.

Now we get down to calculate the reflector using the method which is analogous to Appendix B of [13].

First, consider the adjoint half-space transport problem:

$$\begin{aligned} (\omega\cdot\nu)\partial_z v + v - \overline{v} &= 0, \qquad z>0, \qquad \omega\in\mathbf{S}^{D-1} \\ v(0,\omega) &= 0, \qquad \omega\cdot\nu>0, \\ \overline{(\omega\cdot\nu)v} &= -1, \quad z>0, \end{aligned}$$

where

$$\overline{(\omega\cdot\nu)v} = \frac{1}{|\mathbf{S}^{D-1}|}\int_{\mathbf{S}^{D-1}} f(\omega',\omega)(\omega'\cdot\nu)v d\omega'.$$

Let $\Gamma \in L^\infty(\mathbb{R}_+; L^2(\mathbf{S}^{D-1}, |\omega\cdot\nu|d\omega))$ be the unique solution of (6.4), observe that

$$\begin{aligned}
\frac{d}{dz}\int_{\mathbf{S}^{D-1}} & f(\omega',\omega)(\omega'\cdot\nu)\Gamma(z,\omega')v(z,\omega')d\omega' \\
&= \int_{\mathbf{S}^{D-1}} f(\omega',\omega)(\Gamma(z,\omega') - \overline{\Gamma}(z,\omega))v(z,\omega')d\omega' \\
&\quad -\int_{\mathbf{S}^{D-1}} f(\omega',\omega)\Gamma(z,\omega')(v(z,\omega') - \overline{v}(z,\omega))d\omega' \\
&= -\overline{\Gamma}(z,\omega)\int_{\mathbf{S}^{D-1}} f(\omega',\omega)v(z,\omega')d\omega' \\
&\quad + \overline{v}(z,\omega)\int_{\mathbf{S}^{D-1}} f(\omega',\omega)\Gamma(z,\omega')d\omega' \\
&= 0.
\end{aligned}$$

So by evaluating the quantity $\overline{(\omega\cdot\nu)\Gamma v}$ at $z=0$ and $z\to\infty$, one has

$$\frac{1}{|\mathbf{S}^{D-1}|}\int_{\mathbf{S}_\nu^-} f(\omega',\omega)(\omega'\cdot\nu)v(0,\omega')d\omega' = \overline{(\omega\cdot\nu)v}\Lambda_\nu(G). \tag{6.6}$$

The reasons for the equation (6.6) is as follows:

$$\begin{aligned}
\overline{(\omega\cdot\nu)\Gamma v}|_{z=0} &= \frac{1}{|\mathbf{S}^{D-1}|}\int_{\mathbf{S}^{D-1}} (\omega'\cdot\nu)G(\omega')v(0,\omega')f(\omega',\omega)d\omega' \\
&= \frac{1}{|\mathbf{S}^{D-1}|}\int_{\mathbf{S}_\nu^-} (\omega'\cdot\nu)G(\omega')v(0,\omega')f(\omega',\omega)d\omega' \qquad \text{for } \ v(0,\omega)=0
\end{aligned}$$

when $\nu\cdot\omega > 0$.

And

$$\overline{(\omega\cdot\nu)\Gamma v}|_{z\to\infty} = \overline{(\omega\cdot\nu)v}\Lambda_\nu(G).$$

Then the equation (6.6) leads to the formula

$$\Lambda_\nu(G) = \frac{1}{|\mathbf{S}^{D-1}|}\int_{\mathbf{S}_\nu^-} |\omega'\cdot\nu|G(\omega')v(0,\omega')f(\omega',\omega)d\omega'$$

Now we define the H-function $H_\nu(\omega) = C\cdot v(0,\omega)$ where $C = (\overline{(\omega\cdot\nu)^2})^{\frac{1}{2}}$

Consider the next function

$$u(z,\omega) = (\omega\cdot\nu)\Gamma(z,\omega) + \int_0^z \overline{\Gamma}(s,\omega)ds,$$

it satisfies

$$\begin{aligned}
-(\omega\cdot\nu)\partial_z u + u - \overline{u} &= 0, \qquad z>0, \qquad \omega\in\mathbf{S}^{D-1} \\
u(0,\omega) &= (\omega\cdot\nu)G(\omega), \quad \omega\cdot\nu<0, \\
\overline{(\omega\cdot\nu)u} &= C^2\Lambda_\nu(G), \quad z>0,
\end{aligned}$$

Let $w\in L^\infty(\mathbb{R}_+; L^2(\mathbf{S}^{D-1}, |\omega\cdot\nu|d\omega))$ be the solution of

$$\begin{aligned}
-(\omega\cdot\nu)\partial_z w + w - \overline{w} = 0, \quad z>0, \ \ \omega\in\mathbf{S}^{D-1}, \\
w(0,\omega) = (\omega\cdot\nu)G(\omega), \quad \omega\cdot\nu<0.
\end{aligned}$$

It must also verify the condition $\overline{(\omega\cdot\nu)w} = 0$ for all $z>0$.

Indeed, by averaging over $\mathbf{S}^{D-1}$ the equations for w and $(\omega\cdot\nu)w$, one finds that

$$\overline{(\omega\cdot\nu)w} = const \quad \text{and} \quad \frac{d}{dz}\overline{(\omega\cdot\nu)^2 w} = \overline{(\omega\cdot\nu)w}$$

Hence the function $u-w$ satisfies

$$\begin{aligned} -(\omega\cdot\nu)\partial_z(u-w) + (u-w) - \overline{(u-w)} &= 0, \qquad z>0, \qquad \omega\in\mathbf{S}^{D-1} \\ (u-w)(0,\omega) &= 0, \quad \omega\cdot\nu<0, \\ \overline{(\omega\cdot\nu)(u-w)} &= C^2\Lambda_\nu(G), \quad z>0, \end{aligned}$$

By the uniqueness of the solution of (6.4), we have

$$(u-w)(z,\mathbf{s}_\nu\omega) = C^2\Lambda_\nu(G)v(z,\omega), \tag{6.7}$$

where $\mathbf{s}_\nu(\omega)=\omega-2(\omega\cdot\nu)\nu$.

At $z=0$ and for $\omega\cdot\nu<0$, this relation (6.7) can be recast as

$$\begin{aligned} &-(\omega\cdot\nu)\mathcal{R}G(\omega) - (\mathcal{R}_\nu(\omega\cdot\nu)G)(\omega) \\ &\quad = \frac{1}{|\mathbf{S}^{D-1}|}H_\nu(\omega)\int_{\mathbf{S}_\nu^-}|\omega'\cdot\nu|H_\nu(\omega')G(\omega')f(\omega',\omega)d\omega'. \end{aligned} \tag{6.8}$$

The reasons for (6.8) are:

$$\begin{aligned} u(0,\omega)=(\omega\cdot\nu)\Gamma(0,\omega) \quad &\Longrightarrow \quad u(z,\mathbf{s}_\nu(\omega)) = -(\omega\cdot\nu)\mathcal{R}_\nu G(\omega) \\ w(0,\omega)=(\omega\cdot\nu)G(\omega) \quad &\Longrightarrow \quad w(z,\mathbf{s}_\nu(\omega)) = -(\mathcal{R}_\nu(\omega\cdot\nu)G)(\omega) \end{aligned}$$

The relation (6.8) shows that

$$\mathcal{R}_\nu G(\omega) = \frac{1}{|\mathbf{S}^{D-1}|}\int_{\mathbf{S}_\nu^-} r_\nu(\omega,\omega')G(\omega')|\omega'\cdot\nu|f(\omega',\omega)d\omega',$$

where

$$r_\nu(\omega,\omega') = \frac{H_\nu(\omega)H_\nu(\omega')}{|\omega\cdot\nu|+|\omega'\cdot\nu|}$$

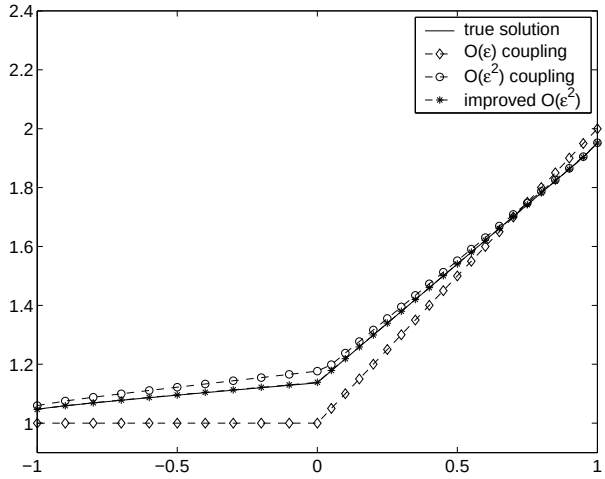

FIGURE 4. Example 1, the compare between the true solution $\overline{\Psi_\varepsilon}$ and the coupling methods' solutions $\overline{\Psi^0}$, $\overline{\Psi_\varepsilon^1}$ and $\overline{\tilde{\Psi}_\varepsilon^1}$. $\varepsilon=0.1$.

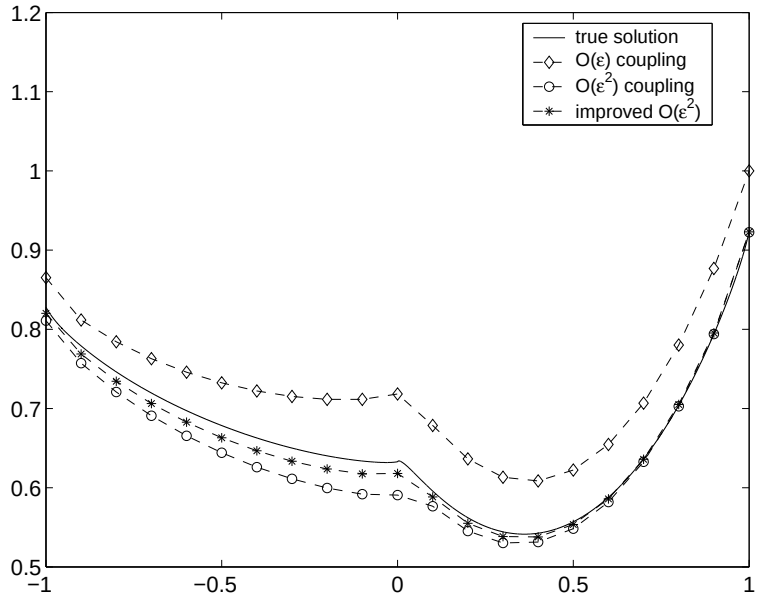

FIGURE 5. Example 2, the compare between the true solution $\overline{\Psi_\varepsilon}$ and the coupling methods' solutions $\overline{\Psi^0}$, $\overline{\Psi_\varepsilon^1}$ and $\overline{\tilde{\Psi}_\varepsilon^1}$. $\varepsilon = 0.1$.

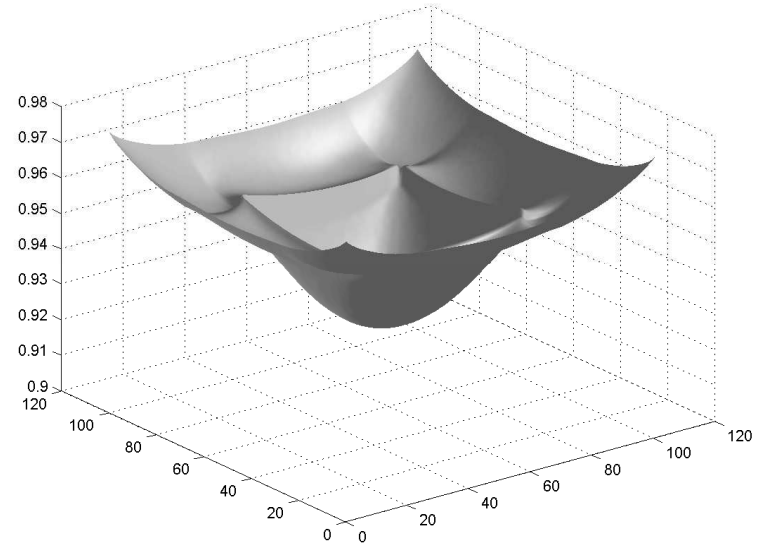

FIGURE 6. Example 3, the numerical density distribution $\overline{\Psi^2}$ by the O(ε) domain decomposition method. $h = 0.01$

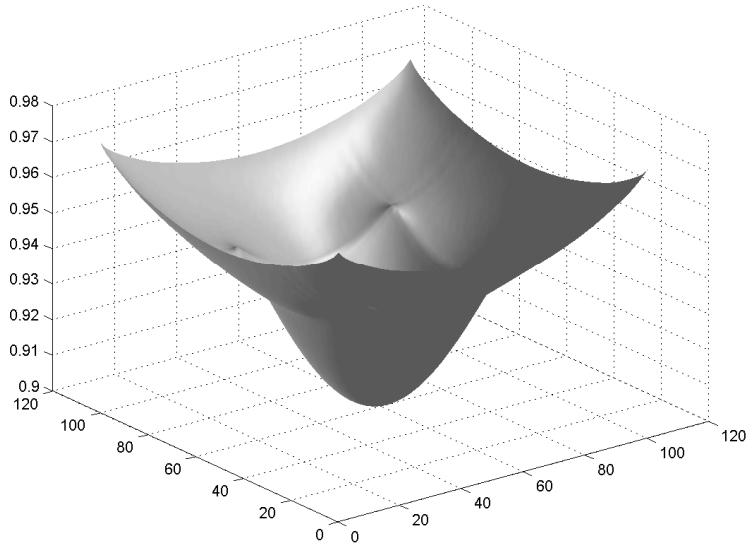

FIGURE 7. Example 3, the numerical density distribution result $\overline{\Psi_\varepsilon}$ by solving directly the original problem.

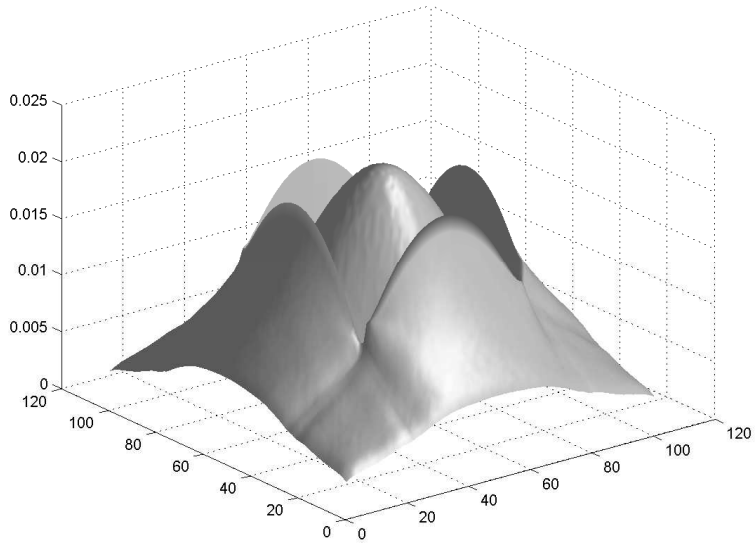

FIGURE 8. Example 3, the error between Figures 6 and 7.

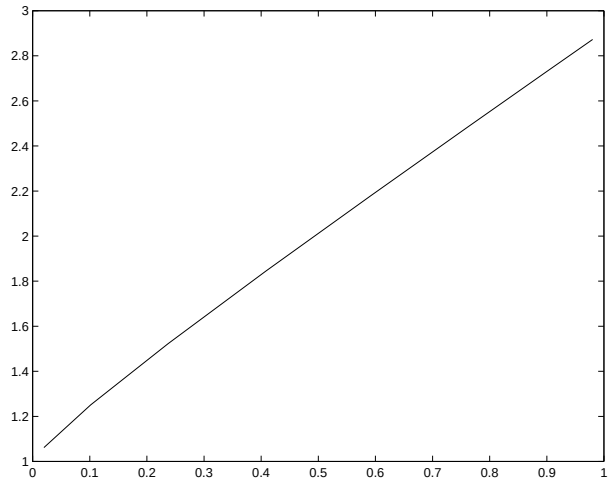

FIGURE 9. the H-function's curve in one-dimensional problem.

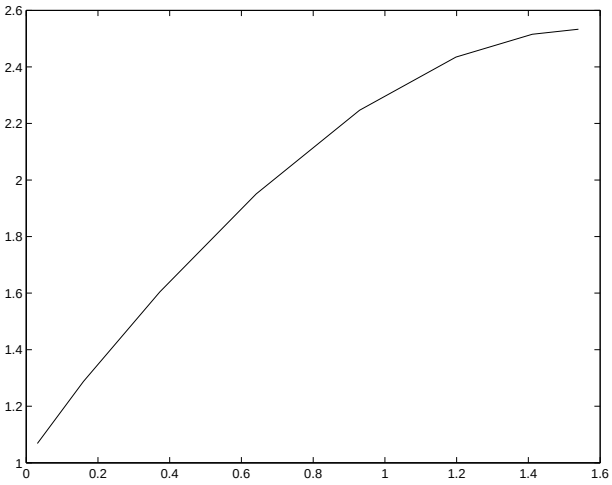

FIGURE 10. the H-function's curve in two-dimensional problem.

REFERENCES

[1] G. Bal, Y. Maday, *Coupling of transport and diffusion models in linear transport theory*, Math. Modeling and Numer. Anal. **36** (2002), 69–86.

[2] C. Bardos, R. Santos, R. Sentis, *Diffusion approximation and computation of critical size*, Trans. Amer. Math. Soc. **284** (1984), 617–649.

[3] A. Bensoussan, J.-L. Lions, G.C. Papanicolaou, *Boundary layers and homogenization of transport processes*, Publ. Res. Inst. Math. Sci. **15** (1979), no. 1, 53–157.

[4] J.-F. Bourgat, P. Le Tallec, B. Perthame, Y. Qiu, *Coupling Boltzmann and Euler equations without overlapping*, in *Domain Decomposition Methods in Science and Engineering (Como, 1992)*, 377–398, Contemp. Math. **157**, Amer. Math. Soc., Providence, RI, 1994.

[5] C. Buet, S. Cordier, B. Lucquin-Desreux, S. Mancini, *Diffusion limit of the Lorentz model: asymptotic preserving schemes*, Math. Modeling and Numer. Anal. **36** (2002), no.4, 631–655.

[6] S. Chandrasekhar, *Radiative Transfer*, Dover, New York, 1960.
[7] R. Dautray, J.L. Lions, *Analyse mathèmatique et calcul numérique pour les sciences et les techniques*, Collection du Commissariat à l'Energie Atomique: Série Scientifique, Masson, Paris, 1985.
[8] P. Degond, C. Schmeiser, *Kinetic boundary layers and fluid-kinetic coupling in semiconductors*, Transport Theory Statist. Phys. **28** (1999), no. 1, 31–55.
[9] S. Dellacherie, *Kinetic fluid coupling in the field of the atomic vapor laser isotopic separation: numerical results in the case of a mono-species perfect gas*, presented at the 23rd International Symposium on Rarefied Gas Dynamics, Whistler (British Columbia), July 2002.
[10] F. Golse, *Applications of the Boltzmann equation within the context of upper atmosphere vehicle aerodynamics*, Computer Meth. in Appl. Mech. and Engineering **75** (1989), 299-316.
[11] F. Golse, *Knudsen layers from a computational viewpoint*, Transp. Theory and Stat. Phys. **21**, (1992), 211–236.
[12] F. Golse, S. Jin and C.D. Levermore, *The Convergence of numerical transfer schemes in diffusive regimes, I. The dicrete-ordinate method*, SIAM J. Num. Anal. **36** (1999), 1333–1369.
[13] François Golse, Shi Jin and C.David Levermore, *A Domain decomposition analysis for a two-scale linear transport problem*, Math. Model Num. Anal, **37** (2003), 869-892.
[14] M. Günther, P. Le Tallec, J.-P. Perlat, J. Struckmeier, *Numerical modeling of gas flows in the transition between rarefied and continuum regimes. Numerical flow simulation I*, (Marseille, 1997), 222–241, Notes Numer. Fluid Mech., 66, Vieweg, Braunschweig, 1998.
[15] S. Jin and C.D. Levermore, *The Discrete-ordinate method in diffusive regimes*, Transp. Theory and Stat. Phys. **20** (1991), 413–439.
[16] S. Jin and C.D. Levermore, *Fully discrete numerical transfer in diffusive regimes*, Transport Theory Statist. Phys. **22** (1993), 739–791.
[17] A. Klar, *Convergence of alternating domain decomposition schemes for kinetic and aerodynamic equations*, Math. Methods Appl. Sci. **18** (1995), no. 8, 649–670.
[18] A. Klar, *Asymptotic-induced domain decomposition methods for kinetic and drift-diffusion semiconductor equations*, SIAM J. Sci. Comput. **19** (1998), 2032–2050.
[19] A. Klar, H. Neunzert and J. Struckmeier, *Transition from kinetic theory to macroscopic fluid equations: a problem for domain decomposition and a source for new algorithm*, Transp. Theory and Stat. Phys. **29** (2000), 93–106.
[20] A. Klar, N. Siedow, *Boundary layers and domain decomposition for radiative heat transfer and diffusion equations: applications to glass manufacturing process*, European J. Appl. Math. **9** (1998), 351–372.
[21] P. Le Tallec, F. Mallinger, *Coupling Boltzmann and Navier-Stokes equations by half fluxes*, J. Comput. Phys. **136** (1997), 51–67.
[22] P. Le Tallec, M. Tidriri, *Convergence analysis of domain decomposition algorithms with full overlapping for the advection-diffusion problems*, Math. Comp. **68** (1999), 585–606.
[23] M. Tidriri, *New models for the solution of intermediate regimes in transport theory and radiative transfer: existence theory, positivity, asymptotic analysis, and approximations*, J. Stat. Phys. **104** (2001), 291-325.

Received September 2005; revised November 2005.

E-mail address: xyang@math.wisc.edu
E-mail address: Francois.Golse@ens.fr
E-mail address: zhuang@math.tsinghua.edu.cn
E-mail address: jin@math.wisc.edu